Journal of Sound and Vibration (2001) **241**(3), 441–457
doi:10.1006/jsvi.2000.3304, available online at http://www.idealibrary.com on IDEAL®

ACOUSTIC PLANE WAVE INTERACTION WITH A RANDOMLY INHOMOGENEOUS SLAB BOUNDED BY ROUGH SURFACES

J.-Y. Liu and C.-F. Huang

Institute of Undersea Technology, National Sun Yat-sen University Kaoshiung, Kaoshiung 804, *Taiwan, Republic of China. E-mail: jimliu@mail.nsysu.edu.tw*

(*Received* 22 *March* 2000, *and in final form* 8 *August* 2000)

Acoustic plane wave incident upon a fluid slab bounded by rough surfaces, within which the sound-speed distribution is subject to random perturbation, is considered. A theory based upon a boundary perturbation method in conjunction with a formulation derived from Green's function for the coherent field in the random medium has been applied to a typical oceanic environment, to study the coherent reflection from and transmission through the rough-and-random slab. Under the assumption of independence between the randomness of rough surface and that of sound-speed perturbation, the coherent fields may be obtained straightforwardly using formulations compatible with those employed in the existing literature. The reflection and transmission coefficients are then numerically generated for various cases to analyze the effects of surface roughness and medium inhomogeneities. The results have shown that both mechanisms reduce the coherent reflection and transmission coefficients, because of the generation of incoherent scattered fields which in effect are to disperse coherent energy. It is also interesting to note that the variation of the reflection coefficient near the critical angle presents distinctive characteristics for different scattering mechanisms, potentially allowing to identify the dominant one for a particular problem under consideration.

1. INTRODUCTION

This paper considers a plane wave impinging upon a randomly inhomogeneous slab bounded by rough surfaces, within which the distribution of the sound speed is subject to small and random perturbations, while the density is assumed to remain constant. The schematic diagram of the problem is shown in Figure 1. The density is taken to be constant with reference to the fact that in oceans, which are the environment of present concern, the density fluctuation is often much smaller than that of sound speed [1]. The scenario shown in Figure 1 is likely to occur in an oceanic environment; for example, an acoustic wave passing through a region where the distribution of the sound speed is disturbed by oceanographic mixing such as eddies and internal waves [2–4], or by foreign biomass such as deep scattering layer [5]. It is conceivable when an acoustic wave propagates through such a region, it may be attenuated by surface and volume scattering simultaneously, resulting in a further loss of energy in addition to that due to classical mechanisms including geometrical spreading and volumetric absorption. The proposed model may seem too simplistic to fully account for the situations described above; however, the fundamental principles revealed by the present analysis should shed light on the basic mechanisms involved in a more complex system. It is the primary purpose of this paper to understand these basic mechanisms.

0022-460X/01/130441 + 17 $35.00/0

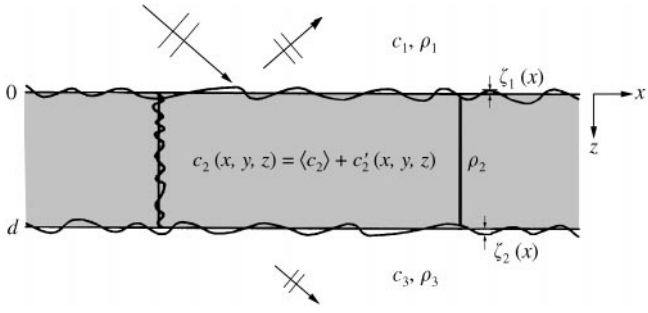

Figure 1. Environmental model: a plane wave incident upon a slab of randomly inhomogeneous medium, within which the sound-speed distribution is subject to a small perturbation.

The effects of medium inhomogeneities on plane wave reflection similar to the present analysis were studied by several authors recently, including a series of papers on plane wave reflection from a surface overlying a medium with continuously varying density and sound speed by Robins [6–8], and several others on reflection from randomly inhomogeneous medium, e.g., by Tang and Frisk [9, 10]. However, in these studies, the interfaces are assumed to be smooth so that the effects of surface roughness have not yet been considered. Recently, the present authors have considered the effects of rough surface on the coherent reflection over a deterministically inhomogeneous layer with continuously varying density and sound speed [11], and randomly inhomogeneous half-space [12]. Furthermore, the incoherent scattered field was also studied [13]. The results from these analyses have shown that the surface roughness presents significant effects on the characteristics of the reflection field. In all of the above analyses, only single-interface (Rayleigh) scattering was considered. The present study introduces multiple rough interfaces and considers their effects on plane wave reflection and transmission. This seemingly straightforward extension has immediately aroused many concerns relevant to multiple scattering occurring in a reverberation waveguide, a mechanism far more complicated than that for single-interface scattering considered before. In this analysis, we shall derive Green's function and the solutions for the wave field in the random slab, and then employ a formulation that is appropriate to account for the scattering in a random waveguide environment.

In the following sections, we shall first formulate the problem, and then present numerical implementation. Many results for the reflection and transmission coefficients for various statistical parameters characterizing the roughness of the surface and randomness of the medium are generated and analyzed.

2. FORMULATIONS

Consider a monotonic acoustic plane wave with time-dependent $e^{i\omega t}$, propagating in x–z plane, and encountering a fluid slab whose sound speed distribution is subject to small and random perturbation:

$$c_2 = \langle c_2 \rangle + c_2'(\mathbf{r}, z), \tag{1}$$

where $\mathbf{r}$ is the horizontal co-ordinate, $\langle c_2 \rangle$ is the ensemble average over the random medium, and c_2' is the random variation of the sound speed, which is assumed to be zero-mean and small compared with $\langle c_2 \rangle$, i.e., $|c_2'| \ll |\langle c_2 \rangle|$. Furthermore, it is assumed that

the randomness of the sound speed is homogeneous in the horizontal direction. The slab is bounded by two one-dimensional rough surfaces with random elevation $z = \zeta_i(x)$, $(i = 1, 2)$, which are also assumed to be zero-mean, and whose magnitude and slope are small compared to wavelength. It is to be pointed out in advance that, despite the fact that the medium randomness is three-dimensional, the very assumption of randomness being horizontally homogeneous makes the ensemble averages of the reflection and transmission fields two-dimensional, i.e., independent of y co-ordinate; this shall greatly simplify the future analysis.

Under the above assumptions, the Helmholtz equations and the boundary conditions may be shown to satisfy the following equations:

$$\nabla^2 p_1 + k_1^2 p_1 = 0, \quad \nabla^2 p_2 + \langle k_2 \rangle^2 (1 - \varepsilon) p_2 = 0, \quad \nabla^2 p_3 + k_3^2 p_3 = 0, \tag{2–4}$$

$$p_1(\mathbf{r}, \zeta_1) = p_2(\mathbf{r}, \zeta_1), \quad w_1(\mathbf{r}, \zeta_1) = w_2(\mathbf{r}, \zeta_1), \tag{5, 6}$$

$$p_2(\mathbf{r}, \zeta_2) = p_3(\mathbf{r}, \zeta_2), \quad w_2(\mathbf{r}, \zeta_2) = w_3(\mathbf{r}, \zeta_2), \tag{7, 8}$$

where p_i, w_i, $k_i = \omega/c_i$ are, respectively, the acoustic pressure, vertical displacement, and wavenumber in the ith medium, and the parameter ε in equation (3), is defined as $\varepsilon = -2c_2'/\langle c_2 \rangle$. The coefficient for p_2 in equation (3) is obtained by invoking the assumption that c_2' is much smaller than $\langle c_2 \rangle$, and through the following approximation:

$$k_2^2 = \left(\frac{\omega}{\langle c_2 \rangle + c'} \right)^2 \simeq \left[\frac{\omega}{\langle c_2 \rangle} \left(1 - \frac{\varepsilon}{2} \right) \right]^2 \simeq \langle k_2 \rangle^2 (1 - \varepsilon). \tag{9}$$

It should be noted that c_2' embedded in ε in equation (3) and ζ_1, ζ_2 in equations (5–8) are random parameters, and in the most general case they may be correlated. However, in this study we shall assume that each randomness originates from different physical processes, and therefore they are taken to be statistically independent.

The approach for the solution of the problem shall be based upon the self-consistent formulation developed by Kuperman and Schmidt [14, 15], in which the effects of rough-surface scattering may be accounted for by introducing several boundary operators whose components only involve the corresponding undisturbed and uniform problem. However, in the present analysis, the acoustic properties in the slab are randomly inhomogeneous. In this regard, it has been shown and discussed by Liu and Huang [12] that, to obtain the solution of the coherent reflection and transmission coefficients, it is sufficient to first derive the leading-order solution in the random medium, and then employ the self-consistent formulation for rough-surface scattering; this is the syllabus to be followed below.

2.1. GREEN'S FUNCTION AND MEAN-FIELD SOLUTION IN THE RANDOM SLAB

Here, we shall first derive the solution for wave propagation in the random slab. Following the common practice of scattering analysis on wave in random media, the solution for equation (3) may be decomposed into a coherent mean field $\langle p_2 \rangle$, and incoherent scattered field p_2^s:

$$p_2 = \langle p_2 \rangle + p_2^s, \tag{10}$$

where it is assumed that $|p_2^s| \ll |\langle p_2 \rangle|$. Substituting equation (10) into equation (3), and then taking the ensemble average results in the wave equation for the mean field:

$$\nabla^2 \langle p_2 \rangle + \langle k_2 \rangle^2 \langle p_2 \rangle = - \langle k_2 \rangle^2 \langle \varepsilon p_2^s \rangle. \tag{11}$$

Furthermore, subtracting equations (11) from (3), then dropping the higher order terms, yields the wave equation for the scattered field:

$$\nabla^2 p_2^s + \langle k_2 \rangle^2 p_2^s = - \varepsilon \langle k_2 \rangle^2 \langle p_2 \rangle. \tag{12}$$

It is noted that the term on the right-hand side of equation (11) is being retained so that the system is able to maintain consistence with the fact that the energy extracted from the coherent field by scattering may be appropriately accounted for.

Applying Green's formula in equation (12), and then substituting the resulting formulation into equation (11) yields the equations for mean field and scattered field, respectively, given by

$$\nabla^2 \langle p_2 \rangle + \langle k_2 \rangle^2 \langle p_2 \rangle = - \frac{\langle k_2 \rangle^4}{4\pi} \int_{V(\mathbf{R}')} \langle \varepsilon(\mathbf{R}') \varepsilon(\mathbf{R}) \rangle \langle p_2(\mathbf{R}') \rangle G_2(\mathbf{R}; \mathbf{R}') \, \mathrm{d}V(\mathbf{R}'), \tag{13}$$

$$p_2^s(\mathbf{R}) = \frac{\langle k_2 \rangle^2}{4\pi} \int_{V(\mathbf{R}')} \varepsilon(\mathbf{R}') \langle p_2(\mathbf{R}') \rangle G_2(\mathbf{R}; \mathbf{R}') \, \mathrm{d}V(\mathbf{R}'), \tag{14}$$

where $\mathbf{R} = (\mathbf{r}, z)$, and $G(\mathbf{R}; \mathbf{R}')$ is Green's function in the random slab. It is seen that the mean field is governed by an integro-differential equation, and the scattered field, which is excited by the mean field, may be derived from equation once the mean field is obtained. In the present study, we are primarily concerned with the coherent field so that the solution of equation (13) is in order.

Equation (13) shows that, in order to obtain the solution for the mean field, it is necessary to derive Green's function in the slab, which in the present case requires one to solve the following system of equations:

$$(\nabla^2 + k_1^2) G_1(\mathbf{R}; \mathbf{R}') = 0, \quad z < 0, \tag{15}$$

$$(\nabla^2 + \langle k_2 \rangle^2) G_2(\mathbf{R}; \mathbf{R}') = - 4\pi \delta(\mathbf{R} - \mathbf{R}'), \quad 0 < z < d, \tag{16}$$

$$(\nabla^2 + k_3^2) G_3(\mathbf{R}; \mathbf{R}') = 0, \quad z > d \tag{17}$$

with the boundary conditions:

$$G_1(\mathbf{R}; \mathbf{R}')|_{z=0} = G_2(\mathbf{R}; \mathbf{R}')|_{z=0}, \tag{18}$$

$$\frac{1}{\rho_1} \frac{\partial}{\partial z} G_1(\mathbf{R}; \mathbf{R}')|_{z=0} = \frac{1}{\rho_2} \frac{\partial}{\partial z} G_2(\mathbf{R}; \mathbf{R}')|_{z=0}, \tag{19}$$

$$G_2(\mathbf{R}; \mathbf{R}')|_{z=d} = G_3(\mathbf{R}; \mathbf{R}')|_{z=d}, \tag{20}$$

$$\frac{1}{\rho_2} \frac{\partial}{\partial z} G_2(\mathbf{R}; \mathbf{R}')|_{z=d} = \frac{1}{\rho_3} \frac{\partial}{\partial z} G_3(\mathbf{R}; \mathbf{R}')|_{z=d}, \tag{21}$$

Without loss of generality, the solution in each layer may be expressed by generalized Fourier integral:

$$G_1(\mathbf{R};\mathbf{R}') = \int_0^\infty A e^{ik_{z,1}z} J_0(k_r r) k_r \, dk_r, \tag{22}$$

$$G_2(\mathbf{R};R') = \int_0^\infty \frac{i}{k_{z,2}} (B e^{ik_{z,2}z} + C e^{-ik_{z,2}z} + e^{-ik_{z,2}|z-z'|}) J_0(k_r r) k_r \, dk_r, \tag{23}$$

$$G_3(\mathbf{R};R') = \int_0^\infty D e^{-ik_{z,3}(z-d)} J_0(k_r r) k_r \, dk_r, \tag{24}$$

where $k_{z,i} = (\langle k_i \rangle^2 - k_r^2)^{1/2}$ is the vertical wavenumber in the ith layer (for the first and the third layers, the average wavenumber is just the wavenumber itself).

The above system may readily be solved for B and C in G_2 by existing software such as *Mathematica* [16], and the solutions are

$$B = e^{-ik_{z,2}|d-z'|-ik_{z,2}|z'|}(-k_{z,3}\rho_2 + k_{z,2}\rho_3)\frac{\mathscr{D}_1}{\mathscr{D}}, \tag{25}$$

$$C = e^{ik_{z,2}d-ik_{z,2}|d-z'|-ik_{z,2}|z'|}(k_{z,2}\rho_1 - k_{z,1}\rho_2)\frac{\mathscr{D}_2}{\mathscr{D}} \tag{26}$$

with $\mathscr{D}$, $\mathscr{D}_1$, and $\mathscr{D}_2$ given by

$$\begin{aligned}\mathscr{D} = {} & k_{z,2}k_{z,3}\rho_1\rho_2 + e^{2ik_{z,2}d}k_{z,2}k_{z,3}\rho_1\rho_2 - k_{z,1}k_{z,3}\rho_2^2 + e^{2ik_{z,2}d}k_{z,1}k_{z,3}\rho_2^2 \\ & - k_{z,2}^2\rho_1\rho_3 + e^{2ik_{z,2}d}k_{z,2}^2\rho_1\rho_3 + k_{z,1}k_{z,2}\rho_2\rho_3 + e^{2ik_{z,2}d}k_{z,1}k_{z,2}\rho_2\rho_3,\end{aligned} \tag{27}$$

$$\mathscr{D}_1 = e^{ik_{z,2}d+ik_{z,2}|z'|}(k_{z,2}\rho_1 + k_{z,1}\rho_2) + e^{ik_{z,2}|d-z'|}(k_{z,2}\rho_1 - k_{z,1}\rho_2), \tag{28}$$

$$\mathscr{D}_2 = e^{ik_{z,2}d+ik_{z,2}|d-z'|}(k_{z,3}\rho_1 + k_{z,2}\rho_3) - e^{ik_{z,2}|z'|}(k_{z,3}\rho_2 - k_{z,2}\rho_3). \tag{29}$$

On the other hand, the solution of the mean field also depends upon the spatial correlation of the sound-speed randomness, as shown in equation (13). In this regard, the medium is assumed to be anisotropic, with high correlation in the horizontal direction and low correlation in the vertical direction, so that the correlation function may be expressed as [17, 18]:

$$\langle \varepsilon(\mathbf{R}_1)\varepsilon(\mathbf{R}_2)\rangle = 4\sigma^2 N(\bar{r})M(\bar{z}), \tag{30}$$

where σ represents r.m.s. randomness of $c_2'/\langle c_2\rangle$, and $\bar{r} = |\mathbf{r}_1 - \mathbf{r}_2|$, $\bar{z} = |z_1 - z_2|$; $N(\bar{r})$ and $M(\bar{z})$ are, respectively, the horizontal and vertical correlation functions of the random sound-speed variations. For practical purposes, the horizontal and vertical correlations are taken to be Gaussian and Dirac–delta function, respectively, i.e.,

$$N(\bar{r}) = e^{-\bar{r}^2/L_0^2}, \tag{31}$$

$$M(\bar{z}) = z_0\delta(\bar{z}), \tag{32}$$

where L_0 is the horizontal correlation distance, and z_0 is a constant representing the "energy" content.

Substituting equation (30) into equation (13), the equation governing the mean field becomes

$$\nabla^2\langle p_2\rangle + \langle k_2\rangle^2\langle p_2\rangle = -\frac{\langle k_2\rangle^4\sigma^2}{\pi}\int_{V(\mathbf{R}')} N(\bar{r}')M(\bar{z}')\langle p_2(\mathbf{R}')\rangle G_2(\mathbf{R};\mathbf{R}')\,\mathrm{d}V(\mathbf{R}'). \quad (33)$$

Furthermore, inserting equation (32) into equation (33), and considering the fact that the incoming plane wave lies on x–z plane and the roughness is one dimensional so that there is no out-of-plane component for the mean field, the solution for $\langle p_2\rangle$, being independent of y, may be expressed as

$$\langle p_2(x, z)\rangle = \mathrm{e}^{-\mathrm{i}k_{r,0}x}q(z). \quad (34)$$

Substituting equations (31), (32) and (34) into equation (33), and assuming that $z_0 \ll \lambda$, where λ is the acoustic wavelength, equation (33) may be analytically simplified to become [10]

$$\left[\frac{\mathrm{d}^2}{\mathrm{d}z^2} + (\langle k_2\rangle^2 - k_{r,0}^2)\right]q(z) = -2\langle k_2\rangle^4\sigma^2 z_0 q(z)\int_0^\infty N(\xi)\mathrm{J}_0(k_{r,0}\xi)G_2(\xi, z; z')\xi\,\mathrm{d}\xi. \quad (35)$$

The above equation was derived under the assumptions that $q(z')$ and $G_2(x, z; x', z')$ embedded in equation (33) are slowly varying functions over z' so that it was set to be equal to z, and then subsequently taken out of integral with respect to z'.

To further simplify the formulation, with $z' = z$, equation (23) is rewritten as

$$G_2(\mathbf{R};\mathbf{R}') = \int_0^\infty \frac{\mathrm{i}}{k_{z,2}}(B_1\mathrm{e}^{2\mathrm{i}k_{z,2}z} + C_1\mathrm{e}^{-2\mathrm{i}k_{z,2}z} + B_2 + 1)\mathrm{J}_0(k_r r)k_r\,\mathrm{d}k_r, \quad (36)$$

where

$$B_1 = (k_{z,2}\rho_1 + k_{z,1}\rho_2)(-k_{z,3}\rho_2 + k_{z,2}\rho_3)\frac{1}{\mathscr{D}}, \quad (37)$$

$$C_1 = (k_{z,2}\rho_1 - k_{z,1}\rho_2)(k_{z,3}\rho_2 + k_{z,2}\rho_3)\frac{\mathrm{e}^{2\mathrm{i}k_{z,2}d}}{\mathscr{D}}, \quad (38)$$

$$B_2 = (k_{z,2}\rho_1 - k_{z,1}\rho_2)(-k_{z,3}\rho_2 + k_{z,2}\rho_3)\frac{2}{\mathscr{D}}. \quad (39)$$

Further substitution of equation (31) and (36) into equation (35), and via some algebraic manipulations, a non-homogeneous second order ordinary differential equation results:

$$\frac{\mathrm{d}^2q}{\mathrm{d}z^2} + \eta^2 q = -\mathscr{F}(z)q, \quad (40)$$

where

$$\mathscr{F}(z) = 2\langle k_2\rangle^4\sigma^2 z_0\int_0^\infty \frac{\mathrm{i}}{k_{z,2}}\mathscr{H}(k_r, k_{r,0})(B_1\mathrm{e}^{2\mathrm{i}k_{z,2}z} + C_1\mathrm{e}^{-2\mathrm{i}k_{z,2}z})k_r\,\mathrm{d}k_r \quad (41)$$

with relevant parameters and functions defined as follows:

$$\eta^2 = \langle k_2 \rangle^2 \left[1 - \frac{k_{r,0}^2}{\langle k_2 \rangle^2} + c(k_{r,0}) \right] \tag{42}$$

$$c(k_{r,0}) = 2\langle k_2 \rangle^2 \sigma^2 z_0 \int_0^\infty \frac{\mathrm{i}}{k_{z,2}} \mathscr{H}(k_r, k_{r,0})(B_2 + 1) k_r \, \mathrm{d}k_r \tag{43}$$

$$\mathscr{H}(k_r, k_{r,0}) = \int_0^\infty N(\xi) \mathrm{J}_0(k_{r,0}\xi) \mathrm{J}_0(k_r \xi) \xi \, \mathrm{d}\xi \tag{44}$$

$$= \tfrac{1}{2} L_0^2 \mathrm{e}^{-(k_{r,0}^2 + k_r^2) L_0^2/4} \mathrm{I}_0(k_{r,0} k_r L_0^2/2). \tag{45}$$

Due to the fact that $|\mathscr{F}(z)| \ll |\eta^2|$, equation (40) may be solved by first dropping the right-hand side to obtain the first-iteration solution, and then solving the full equation by the method of variation of parameter to yield [19]

$$q(z) = A_1 q_1(z) + A_2 q_2(z), \tag{46}$$

where

$$q_1(z) = \mathrm{e}^{-\mathrm{i}\eta z} - \frac{1}{2\mathrm{i}\eta} \left[\mathrm{e}^{-\mathrm{i}\eta z} \int_z^0 \mathscr{F}(z') \, \mathrm{d}z' + \mathrm{e}^{\mathrm{i}\eta z} \int_d^z \mathscr{F}(z') \mathrm{e}^{-2\mathrm{i}\eta z'} \, \mathrm{d}z' \right], \tag{47}$$

$$q_2(z) = \mathrm{e}^{\mathrm{i}\eta z} - \frac{1}{2\mathrm{i}\eta} \left[\mathrm{e}^{-\mathrm{i}\eta z} \int_z^0 \mathscr{F}(z') \mathrm{e}^{2\mathrm{i}\eta z'} \, \mathrm{d}z' + \mathrm{e}^{\mathrm{i}\eta z} \int_d^z \mathscr{F}(z') \, \mathrm{d}z' \right]. \tag{48}$$

This is the desired solution for the wave field inside the slab. Finally, since the upper and lower media are homogeneous, their solutions may be expressed as

$$p_1(x, z) = \mathrm{e}^{-\mathrm{i}(k_{r,0} x + k_{z,1} z)} + \langle \mathscr{R} \rangle \mathrm{e}^{-\mathrm{i}(k_{r,0} x - k_{z,1} z)}, \tag{49}$$

$$p_3(x, z) = \langle \mathscr{T} \rangle \mathrm{e}^{-\mathrm{i}[k_{r,0} x + k_{z,3}(z - d)]}. \tag{50}$$

2.2. REFLECTION AND TRANSMISSION COEFFICIENTS

Having obtained the solutions for wave propagation in all three layers, it is now appropriate to consider wave interaction with the rough surfaces. Here, as mentioned previously, we shall employ the method of boundary perturbation developed by Kuperman and Schmidt [15], in which the effects of rough surface scattering on the coherent field may be accounted for by modifying the boundary conditions corresponding to the case of smooth interface. Since the details of the derivation may be found in reference [15], only the final formulation is presented here.

To apply the Kuperman–Schmidt theory, it is necessary to first establish the linear system for the unknown amplitudes of wave components in various layers for the case of smooth interfaces. With respect to this, it may be shown that, by invoking the boundary

conditions stipulated by the physical requirements of continuities of pressure and vertical displacement, the same as those shown in equations (18)–(21), the linear system may be conveniently expressed as

$$\mathscr{B}(k_{r,0})\chi(k_{r,0}) = \mathscr{C}(k_{r,0}), \tag{51}$$

where

$$\mathscr{B}(k_{r,0}) = \begin{bmatrix} 1 & -\frac{1}{2i\eta}(2i\eta - h_1) & -\frac{1}{2i\eta}(2i\eta - h_2) & 0 \\ \frac{ik_{z,1}}{\rho_1\omega^2} & \frac{1}{2\rho_2\omega^2}(2i\eta + h_1) & -\frac{1}{2\rho_2\omega^2}(2i\eta - h_2) & 0 \\ 0 & \frac{e^{-i\eta d}}{2i\eta}(2i\eta - h_2) & \frac{e^{i\eta d}}{2i\eta}(2i\eta - h_3 e^{-2i\eta d}) & -1 \\ 0 & \frac{e^{-i\eta d}}{2\rho_2\omega^2}(2i\eta - h_2) & \frac{e^{i\eta d}}{2\rho_2\omega^2}(2i\eta + h_3 e^{-2i\eta d}) & \frac{ik_{z,3}}{\rho_3\omega^2} \end{bmatrix}, \tag{52}$$

$$\chi = [\langle\mathscr{R}\rangle, A_1, A_2, \langle\mathscr{T}\rangle]^{\mathrm{T}}, \tag{53}$$

$$\mathscr{C} = \left[-1, \frac{ik_{z,1}}{\rho_1\omega^2}, 0, 0\right]^{\mathrm{T}} \tag{54}$$

with h_1, h_2 and h_3 being functions of $k_{r,0}$, and given by

$$\begin{bmatrix} h_1 \\ h_2 \\ h_3 \end{bmatrix} = \int_d^0 \mathscr{F}(z') \begin{bmatrix} e^{-2i\eta z'} \\ 1 \\ e^{2i\eta z'} \end{bmatrix} dz' \tag{55}$$

$$= \int_0^\infty \mathscr{H}^*(k_r, k_{r,0}) \begin{bmatrix} B_1 \frac{e^{2id(k_{z,2}-\eta)} - 1}{k_{z,2} - \eta} - C_1 \frac{e^{-2id(k_{z,2}+\eta)} - 1}{k_{z,2} + \eta} \\ B_1 \frac{e^{2ik_{z,2}d} - 1}{k_{z,2}} - C_1 \frac{e^{-2ik_{z,2}d} - 1}{k_{z,2}} \\ B_1 \frac{e^{2id(k_{z,2}+\eta)} - 1}{k_{z,2} + \eta} - C_1 \frac{e^{-2id(k_{z,2}-\eta)} - 1}{k_{z,2} - \eta} \end{bmatrix} k_r \, dk_r, \tag{56}$$

where $\mathscr{H}^*(k_r, k_{r,0}) = -(\langle k_2\rangle^4\sigma^2 z_0/k_{z,2})\mathscr{H}(k_r, k_{r,0})$.

For the case of rough boundaries, equation (51) must be modified to account for the random elevation and rotation of the roughness. Through lengthy and cumbersome derivations, the modified boundary condition is [15]

$$\left(\mathscr{B}(k_{r,0}) + \frac{\langle\zeta^2\rangle}{2}\frac{\partial^2\mathscr{B}(k_{r,0})}{\partial z^2} + \mathscr{I}(k_{r,0})\right)\chi(k_{r,0}) = \mathscr{C}(k_{r,0}), \tag{57}$$

where

$$\mathscr{I}(k_{r,0}) = -\frac{\langle\zeta^2\rangle}{\sqrt{2\pi}}\int \mathrm{d}q P(q-k_{r,0})\left(\frac{\partial\mathscr{B}(q)}{\partial z} - \mathrm{i}(k_{r,0}-q)\mathscr{B}_s(q)\right)$$
$$\times\mathscr{B}^{-1}(q)\left(\frac{\partial\mathscr{B}(k_{r,0})}{\partial z} - \mathrm{i}(q-k_{r,0})\mathscr{B}_s(k_{r,0})\right). \tag{58}$$

The matrix $\mathscr{B}_s(k_{r,0})$ representing the effect of surface orientation of the rough surface may be derived as follows:

$$\mathscr{B}_s(k_{r,0}) = \frac{\mathrm{i}k_{r,0}}{\rho_2\omega^2}\begin{bmatrix} 0 & 0 & 0 & 0 \\ \dfrac{\rho_2}{\rho_1} & -1+\dfrac{h_1}{2\mathrm{i}\eta} & -1+\dfrac{h_2}{2\mathrm{i}\eta} & 0 \\ 0 & 0 & 0 & 0 \\ 0 & \left(\mathrm{e}^{-\mathrm{i}\eta d}-\dfrac{\mathrm{e}^{-\mathrm{i}\eta d}h_2}{2\mathrm{i}\eta}\right) & \left(\mathrm{e}^{\mathrm{i}\eta d}-\dfrac{\mathrm{e}^{-\mathrm{i}\eta d}h_3}{2\mathrm{i}\eta}\right) & -\dfrac{\rho_2}{\rho_3} \end{bmatrix}. \tag{59}$$

Other operators relevant to the derivatives of the matrix $\mathscr{B}(k_{r,0})$ appearing in equations (57) and (58) are derived and presented in Appendix A. The power spectrum for the rough surface embedded in equation (58) is also taken to be Gaussian for convenience:

$$P(k) = \sqrt{2\pi}\ell\,\mathrm{e}^{-k^2\ell^2/2}. \tag{60}$$

Here, ℓ represents the correlation length of the roughness. The linear system, equation (51), may be solved for $\langle\mathscr{R}\rangle$ and $\langle\mathscr{T}\rangle$ to obtain the coherent reflection coefficient and transmission coefficient.

3. EXAMPLES AND DISCUSSION

In this section, we shall apply the above formulation to several examples to demonstrate and discuss the results of coherent reflection and transmission coefficients under the effects of various controlling parameters of the problem. In particular, attention is given to the parameters characterizing the present analysis, which are the randomness inside the slab represented by σ, and the roughness over the interfaces represented by r.m.s. roughness $\langle\zeta^2\rangle^{1/2}$. Although the spatial correlation of both the medium randomness and surface roughness may also affect the characteristics of the sound fields (reflection and transmission), it has been demonstrated by Liu and Huang [11] that, as far as the coherent fields are concerned, the spatial correlation, which is important for the scattered field, may only produce a minor effect, so that it is not to be discussed here. The properties of the scattering field is intended to be analyzed in a future paper in relation to the issues of surface and/or volume reverberation in a waveguide propagation.

Here, we consider a plane wave propagating in an oceanic environment, and encountering a randomly inhomogeneous region. Typical values of parameters are chosen as follows:

$$c_1,\, c_3 = 1500\ \mathrm{m/s}, \quad \langle\zeta^2\rangle^{1/2} = 0{\cdot}4\ \mathrm{m},$$

$$\rho_1,\, \rho_3 = 1000\ \mathrm{kg/m^3}, \quad \ell = 10\ \mathrm{m},$$

$$\langle c_2 \rangle = 1800 \text{ m/s}, \quad z_0 = 1 \text{ m},$$

$$\rho_2 = 1300 \text{ kg/m}^3, \quad L_0 = 5 \text{ m},$$

$$d = 20 \text{ m}, \quad \sigma = 0{\cdot}15.$$

The values of frequency and the acoustic properties of the slab or the lower medium may vary according to the purpose of analysis, and will be stated in the caption when it becomes necessary. It is to be stressed here that the numerics chosen for the parameters/variables should be within the limitations of the theories for surface and volume scattering, and are primarily intended to reveal the fundamental mechanisms of the wave interaction, so that they may not be able to cope with those employed in a realistic application.

Figure 2 shows the coherent reflection coefficient for a frequency of 200 Hz due to a slab of average sound speed 1800 m/s and density 1300 kg/m^3 in an oceanic environment. In this case, the ratio of thickness-to-wavelength is about 2·7, an appropriate value to illustrate the characteristics of interaction. The dotted curve is for a smooth-and-uniform slab, which serves as a benchmark solution of the problem. The result indicates that total reflection occurs when the incoming plane wave impinges on the upper interface with a grazing angle lower than the critical angle, which is about $\cos^{-1}(1500/1800) = 33{\cdot}6^\circ$. For grazing angles higher than the critical angle, the reflection coefficient demonstrates an oscillatory behavior, which is due to multiple reflection from the interfaces bounding the slab. The local maxima and minima are resulted when the multiply reflected waves are, respectively, closer and further in phase to each other.

The dashed, dashed-and-dotted, and solid curves in Figure 2 illustrate the coherent reflection, respectively for the case of surface roughness alone, medium randomness alone, and the two combined. It is seen that both the surface roughness and medium randomness cause a reduction of the reflection coefficient. This is readily understood in view of the fact that both perturbations will generate incoherent scattered fields, in effect, to strip coherent energy from the incoming wave. It also shows that total reflection no longer exists, in that energy may escape from the coherent field by either rough-surface scattering or volume scattering. A closer examination may also reveal that the behavior of the curves departing from the benchmark solution (dotted curve) near the critical angle shows a distinctive

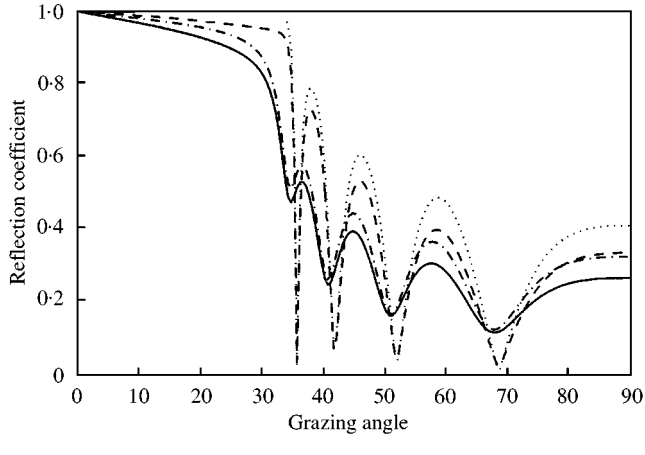

Figure 2. Reflection coefficients: $f = 200$ Hz; $d = 20$ m; (——), $\sigma = 0{\cdot}15$, $\langle \zeta^2 \rangle^{1/2} = 0{\cdot}4$ m; (– –), $\sigma = 0$, $\langle \zeta^2 \rangle^{1/2} = 0{\cdot}4$ m; (·– ·– ·), $\sigma = 0{\cdot}15$, $\langle \zeta^2 \rangle^{1/2} = 0$; (·····), $\sigma = 0$, $\langle \zeta^2 \rangle^{1/2} = 0$.

characteristic for different scattering mechanisms. The dashed-and-dotted curve corresponding to volume scattering demonstrates a "milder" variation than that corresponding to rough-surface scattering which is "sharper" in nature; the former type of variation is similar to that due to medium absorption. As a result, the effect of sound-speed perturbation inside the volume is equivalent to that due to volumetric absorption which has been discussed in some previous literature [20]. Even though either of the scattering mechanisms may become the dominant factor, depending upon the order-of-magnitude of the randomness, the distinct feature near the critical angle is potentially capable of allowing us to identify the dominant mechanism.

Next, the coherent transmission coefficient is considered, which is shown in Figure 3. The result shows that for incident grazing angles higher than the critical angle, the transmission coefficient is significantly reduced by either surface roughness or sound-speed perturbation. It is clear that the transmission coefficient vanishes when the incident grazing angle is lower than the critical angle, in that no energy is being transmitted in this case. It is also noted that the curve representing transmission through a random slab with smooth interface (dashed and dotted) varies much less prominently than that for smooth-and-uniform slab (dotted). In reminiscence of the transmission coefficient corresponding to the Rayleigh problem, it is conceivable that the transmission field in the present analysis is dominated by the first transmitted wave; all other multiply transmitted waves have been significantly damped inside the random slab.

The effect of frequency, equivalently, the thickness-to-wavelength ratio, on the reflection and transmission coefficients is considered in Figures 4 and 5. It is noted that these figures present two sets of curves, corresponding, respectively, to 75 and 150 Hz; each comparing with its corresponding benchmark solution. It is seen that, for a frequency of 150 Hz ($k_1 d = 12{\cdot}6$), the difference between the result for smooth-and-uniform slab (dashed and dotted) and that for rough-and-random slab (solid) is much larger than that for the curves corresponding to 75 Hz ($k_1 d = 6{\cdot}3$) (dotted for rough-and-random slab, and dashed for rough-and-random slab). This indicates that, as the frequency decreases, the effect due to surface roughness and sound-speed perturbation diminishes. This is expected in that, for lower frequency (equivalently, longer wavelength), the interface and the sound-speed distribution inside the slab appear to be smoother and less random, so that the behavior of the reflection and transmission is closer to that for smooth-and-uniform slab.

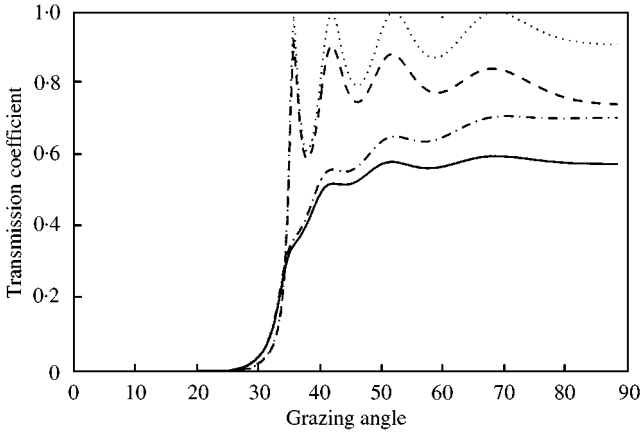

Figure 3. Transmission coefficients: $f = 200$ Hz; $d = 20$ m; (——), $\sigma = 0{\cdot}15$, $\langle \zeta^2 \rangle^{1/2} = 0{\cdot}4$ m; (– – ·), $\sigma = 0$, $\langle \zeta^2 \rangle^{1/2} = 0{\cdot}4$ m; (· – · –), $\sigma = 0{\cdot}15$, $\langle \zeta^2 \rangle^{1/2} = 0$; (· · · · · ·), $\sigma = 0$, $\langle \zeta^2 \rangle^{1/2} = 0$.

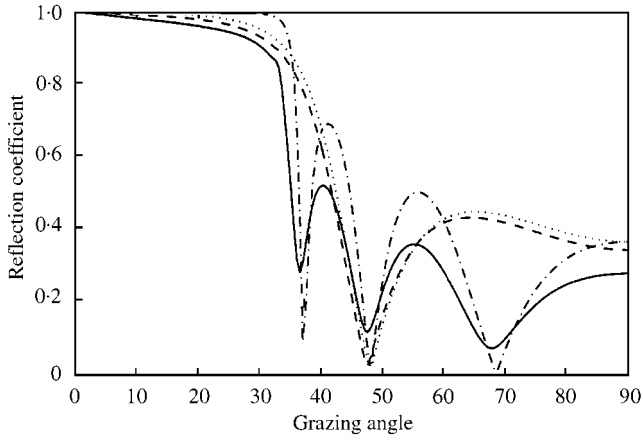

Figure 4. Reflection coefficients for two different frequencies: $f = 75$ Hz; $d = 20$ m; (– –, $\sigma = 0{\cdot}15$, $\langle\zeta^2\rangle^{1/2} = 0{\cdot}4$ m; ·····, $\sigma = 0$, $\langle\zeta^2\rangle^{1/2} = 0$), $f = 150$ Hz; $d = 20$ m; (——, $\sigma = 0{\cdot}15$, $\langle\zeta^2\rangle^{1/2} = 0{\cdot}4$ m; ·–·–, $\sigma = 0$, $\langle\zeta^2\rangle^{1/2} = 0$).

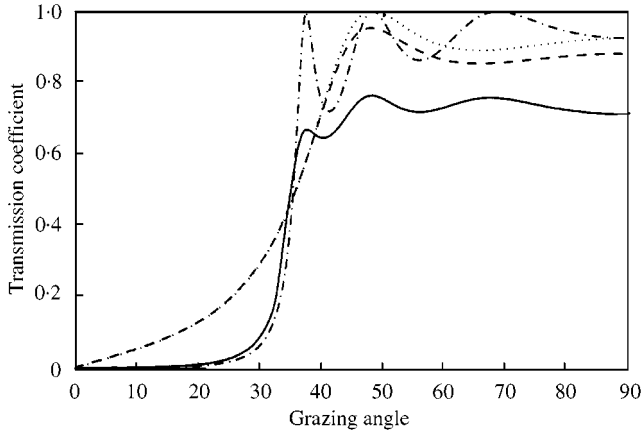

Figure 5. Transmission coefficients for two different frequencies. $f = 75$ Hz; $d = 20$ m; (– –, $\sigma = 0{\cdot}15$, $\langle\zeta^2\rangle^{1/2} = 0{\cdot}4$ m; ·····, $\sigma = 0$, $\langle\zeta^2\rangle^{1/2} = 0$), $f = 150$ Hz; $d = 20$ m; (——, $\sigma = 0{\cdot}15$, $\langle\zeta^2\rangle^{1/2} = 0{\cdot}4$ m; ·–·–·–, $\sigma = 0$, $\langle\zeta^2\rangle^{1/2} = 0$).

Figures 6 and 7 are the results for a slab having smaller sound speed and density than its ambient; the average sound speed and the density are taken, respectively, to be 1400 m/s, and 900 kg/m^3. In this case, since the sound speed in the slab is smaller than that of its ambient, total reflection ceases to exist. Moreover, the results for this case show a slightly different characteristic from those shown previously. In particular, the reflection coefficient under the influence of medium inhomogeneities alone does not present a universal reduction over all grazing angles in comparison with the benchmark solution; this is true particularly for lower grazing angles where the reflection coefficient appears to be larger in some places. The reason for this is the phase interference between multiply reflected waves so that, even though the amplitudes are attenuated, the resulting superposition of various reflected waves may yield higher values in some local intervals. The other properties of these figures are similar to those discussed previously.

Finally, we examine the case where the sound speed and density in the bottom layer are changed to 2000 m/s and 1500 kg/m^3 respectively. In this case, the reflection coefficient

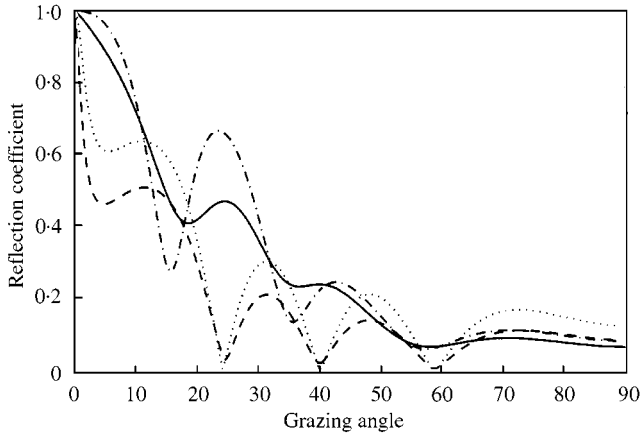

Figure 6. Reflection coefficients for sound speed 1400 m/s and density 900 kg/m^3 in the slab: $f = 200$ Hz, $d = 20$ m; (——), $\sigma = 0{\cdot}15$, $\langle\zeta^2\rangle^{1/2} = 0{\cdot}4$ m; (– –), $\sigma = 0$, $\langle\zeta^2\rangle^{1/2} = 0{\cdot}4$ m; (·–··), $\sigma = 0{\cdot}15$, $\langle\zeta^2\rangle^{1/2} = 0$; (·····), $\sigma = 0$, $\langle\zeta^2\rangle^{1/2} = 0$.

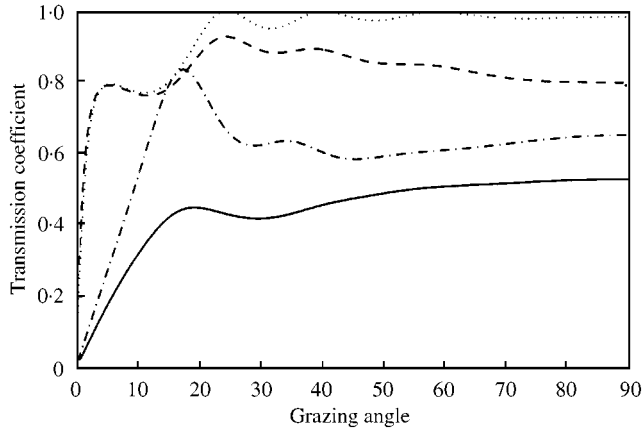

Figure 7. Transmission coefficients for sound speed 1400 m/s and density 900 kg/m^3 in the slab: $f = 200$ Hz, $d = 20$ m; (——), $\sigma = 0{\cdot}15$, $\langle\zeta^2\rangle^{1/2} = 0{\cdot}4$ m; (– –), $\sigma = 0$, $\langle\zeta^2\rangle^{1/2} = 0{\cdot}4$ m; (·–··), $\sigma = 0{\cdot}15$, $\langle\zeta^2\rangle^{1/2} = 0$; (·····), $\sigma = 0$, $\langle\zeta^2\rangle^{1/2} = 0$.

demonstrates a similar behavior to previous results, but the transmission coefficient shows two distinct peaks for smooth-and-uniform (dotted) and rough-and-uniform (dashed) slabs. It is noted that, for the benchmark problem, total reflection occurs for an incident grazing angle less than $\cos^{-1}(1500/2000) = 41{\cdot}4^\circ$ due to the medium contrast between the upper and lower half-spaces; however, the incident wave still penetrates into the slab until $33{\cdot}6^\circ$. Therefore, between these two angles, it is likely that wave interference may result in local minima/maxima, as shown in Figure 8. The transmission coefficient shown in Figure 9 illustrates that scattering inside the slab due to sound-speed perturbation is the dominant factor accounting for the damping of transmission field.

4. CONCLUSIONS AND REMARKS

The purpose of this paper is to demonstrate the interaction between an acoustic plane wave with a random slab bounded by rough interfaces in an oceanic environment. By

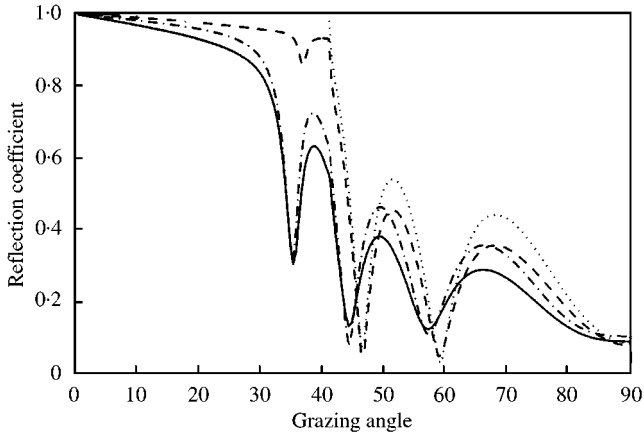

Figure 8. Reflection coefficients for sound speed 2000 m/s and density 1500 kg/m^3 in the lower medium: $f = 200$ Hz, $d = 20$ m; (——), $\sigma = 0{\cdot}15$, $\langle\zeta^2\rangle^{1/2} = 0{\cdot}4$ m; (– –), $\sigma = 0$, $\langle\zeta^2\rangle^{1/2} = 0{\cdot}4$ m; (·–··), $\sigma = 0{\cdot}15$, $\langle\zeta^2\rangle^{1/2} = 0$; (·····), $\sigma = 0$, $\langle\zeta^2\rangle^{1/2} = 0$.

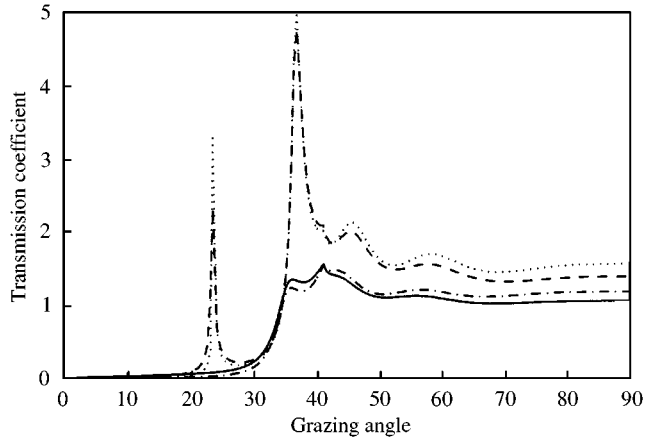

Figure 9. Transmission coefficients for sound speed 2000 m/s and density 1500 kg/m^3 in the lower medium: $f = 200$ Hz, $d = 20$ m; (——), $\sigma = 0{\cdot}15$, $\langle\zeta^2\rangle^{1/2} = 0{\cdot}4$ m; (– –), $\sigma = 0$, $\langle\zeta^2\rangle^{1/2} = 0{\cdot}4$ m; (·–··), $\sigma = 0{\cdot}15$, $\langle\zeta^2\rangle^{1/2} = 0$; (·····), $\sigma = 0$, $\langle\zeta^2\rangle^{1/2} = 0$.

combining a perturbation theory for rough-surface scattering and a Green's formulation for volume scattering due to random sound-speed perturbations, a system of governing equations appropriate for the present analysis is formulated.

Results for the coherent reflection and transmission coefficients were generated and analyzed. It was found that both the coefficients are reduced due to rough surface and volume scattering. However, the characteristics of variation near the critical angle are distinctive with respect to different mechanisms. Furthermore, the effects of thickness-to-wavelength ratio and that of impedance contrast of the media on the reflection and transmission coefficients were studied, and found to be in consistence with compatible results in existing literature.

A few words regarding the theory for scattering from rough surfaces are in order. The theory employed is based upon the boundary perturbation method developed by

Kuperman and Schmidt [15], and was proven to be efficient and satisfactory for scattering from single rough surfaces. However, the multiple scattering which resulted from successive interactions with rough boundaries such as wave propagation in a waveguide bounded by rough surfaces is unable to be appropriately accounted for, therefore, the numerical solution so derived may lead to an overestimation, depending upon the order of magnitude of the roughness. Nonetheless, it has been shown that if the size of roughness is small compared with the wavelength, the error incurred is insignificant. This is further warranted in the present case in that the medium randomness plays a similar role to that of volumetric absorption, which may effectively reduce the error due to the fact that the significance of the multiply reflected waves may be further suppressed, and eventually diminished as the thickness of the slab becomes much larger than the acoustic wavelength.

ACKNOWLEDGMENTS

This work was supported in part by National Science Council of Taiwan, R.O.C. through contract no. NSC89-2611-M-110-012. The authors would like to express their profound thanks for the financial support.

REFERENCES

1. L. A. Chernov 1960 *Wave Propagations in a Random Medium*. New York: McGraw-Hill.
2. L. B. Dozier and F. D. Tappert 1977 *Journal of the Acoustical Society of America* **63**, 352–365. Statistics of normal mode amplitudes in a random ocean: theory.
3. Y. Desaubies 1978 *Journal of the Acoustical Society of America* **64**, 1460–1468. On the scattering of sound by internal waves in the ocean.
4. H. Essen, F. Schirmer and S. Sirkes 1983 *International Journal of Remote Sensing* **4**, 33–47. Acoustic remote sensing of internal waves in shallow water.
5. R. J. Urick 1983 *Principles of Underwater sound*. New York: McGraw-Hill; third edition.
6. A. J. Robins 1990 *Journal of the Acoustical Society of America* **87**, 1546–1552. Reflection of a plane acoustic waves from a layer of varying density.
7. A. J. Robins 1991 *Journal of the Acoustical Society of America* Part 1, **89**, 1686–1696. Reflection of a plane wave from a fluid layer with continuously varying density and sound speed.
8. A. J. Robins 1993 *Journal of the Acoustical Society of America* **93**, 1347–1352. Exact solutions of the Helmholtz equation for plane propagation in a medium with variable density and sound speed.
9. G. V. Frisk 1979 *Journal of the Acoustical Society of America* **66**, 219–234. Inhomogeneous waves and the plane wave reflection coefficient.
10. D. Tang and G. V. Frisk 1991 *Journal of the Acoustical Society of America* **90**, 2751–2756. Plane-wave reflection from a random fluid half-space.
11. J.-Y. Liu, C.-C. Wang and C.-F. Huang 2000 *Journal of Computational Acoustics* **8**, 401–414. Coherent reflection from a rough interface over an inhomogeneous transition fluid layer.
12. J.-Y. Liu and C.-F. Huang *Ocean Engineering*. Acoustic plane-wave reflection from a rough surface over a random fluid half-space, to appear.
13. J.-Y. Liu and C.-F. Huang, *Ocean Engineering*. Acoustic plane-wave scattering from a rough interface over an inhomogeneous transition fluid layer, to appear.
14. W. A. Kuperman 1975 *Journal of the Acoustical Society of America* **58**, 365–370. Coherent component of specular reflection and transmission at a randomly rough two-fluid interface.
15. W. A. Kuperman and H. Schmidt 1986 *Journal of the Acoustical Society of America* **86**, 1511–1522. Self-consistent perturbation approach to rough surface scattering in stratified elastic media.
16. S. Wolfram 1996 *The Mathematica Book*. Cambridge: Cambridge University Press; third edition.

17. A. N. IVAKIN and YU. P. LYSANOV 1981 *Soviet Physics Acoustics* **27**, 61–64. Theory of underwater sound scattering by random inhomogenieties of the bottom.
18. T. YAMAMOTO 1989 *Journal of the Acoustical Society of America* **85** (Suppl. 1), S86. Geoacoustic properties of the seabed sediment critical to acoustic reverberation at 50 to 500 Hz: a preliminary data set.
19. W. E. BOYCE and R. C. DIPRIMA 1997 *Elementary Differential Equations and Boundary Value Problems*. New York: John Wiley; sixth edition.
20. A. WENZEL 1986 *Journal of the Acoustical Society of America* **85** (Suppl), 1511–1522. A method for distinguishing between the attenuation due to scattering and the attenuation due to absorption for waves propagating in a dissipative, randomly inhomogeneous medium.

APPENDIX A

In this appendix, we present the operators $(\partial\mathscr{B}/\partial z)(k_{r,0})$ and $(\partial^2\mathscr{B}/\partial z^2)(k_{r,0})$, which appear in equations (57) and (58). Since the derivation is lengthy it is not presented here. The results of derivation are given as follows:

$$\frac{\partial\mathscr{B}}{\partial z}(k_{r,0}) = \begin{bmatrix} \mathrm{i}k_{z,1} & \mathrm{i}\eta + \dfrac{h_1}{2} & -\mathrm{i}\eta + \dfrac{h_2}{2} & 0 \\ -\dfrac{k_{z,1}^2}{\rho_1\omega^2} & \dfrac{1}{\rho_2\omega^2}\left(\eta^2 + \dfrac{\mathrm{i}\eta h_1}{2} + \mathscr{F}(0)\right) & \dfrac{1}{\rho_2\omega^2}\left(\eta^2 + \dfrac{\mathrm{i}\eta h_2}{2} + \mathscr{F}(0)\right) & 0 \\ 0 & \mathrm{e}^{-\mathrm{i}\eta d}\left(-\mathrm{i}\eta + \dfrac{h_2}{2}\right) & \mathrm{e}^{\mathrm{i}\eta d}\left(\mathrm{i}\eta + \dfrac{h_3}{2}\mathrm{e}^{-\mathrm{i}2\eta d}\right) & \mathrm{i}k_{z,3} \\ 0 & \dfrac{\mathrm{e}^{-\mathrm{i}\eta d}}{\rho_2\omega^2}\left(-\eta^2 - \dfrac{\mathrm{i}\eta h_2}{2} - \mathscr{F}(d)\right) & \dfrac{\mathrm{e}^{-\mathrm{i}\eta d}}{\rho_2\omega^2}\left(-\eta^2 - \dfrac{\mathrm{i}\eta h_3}{2}\mathrm{e}^{-\mathrm{i}2\eta d} - \mathscr{F}(d)\right) & \dfrac{k_{z,3}^2}{\rho_3\omega^2} \end{bmatrix}, \tag{61}$$

$$\frac{\partial^2\mathscr{B}}{\partial z^2}(k_{r,0}) = \begin{bmatrix} -k_{z,1}^2 & \eta^2 + \dfrac{\mathrm{i}\eta h_1}{2} + \mathscr{F}(0) \\ -\dfrac{\mathrm{i}k_{z,1}^3}{\rho_1\omega^2} & -\dfrac{1}{\rho_2\omega^2}\left(\mathrm{i}\eta^3 + \dfrac{\eta^2 h_2(k_{r,0})}{2} + \mathrm{i}\eta\mathscr{F}(0) - \mathscr{F}'(0)\right) \\ 0 & -\mathrm{e}^{-\mathrm{i}\eta d}\left(\eta^2 + \dfrac{\mathrm{i}\eta h_2(k_{r,0})}{2} + \mathscr{F}(d)\right) \\ 0 & \dfrac{\mathrm{e}^{-\mathrm{i}\eta d}}{\rho_2\omega^2}\left(\mathrm{i}\eta^2 - \dfrac{\eta^2 h_2}{2} + \mathrm{i}\eta\mathscr{F}(d) - \mathscr{F}'(d)\right) \end{bmatrix}$$

$$\begin{bmatrix} \eta^2 + \dfrac{\mathrm{i}\eta h_2 + \mathscr{F}(0)}{2} & 0 \\ -\dfrac{1}{\rho_2\omega^2}\left(-\mathrm{i}\eta^3 + \dfrac{\eta^2 h_2}{2} - \mathrm{i}\eta\mathscr{F}(0) - \mathscr{F}'(0)\right) & 0 \\ -\mathrm{e}^{\mathrm{i}\eta d}\left(-\eta^2 + \dfrac{\mathrm{i}\eta h_3}{2}\,\mathrm{e}^{-\mathrm{i}2\eta d} + \mathscr{F}(d)\right) & k_{z,3}^2 \\ \dfrac{\mathrm{e}^{-\mathrm{i}\eta d}}{\rho_2\omega^2}\left(-\mathrm{i}\eta^3 - \dfrac{\eta^2 h_3}{2}\,\mathrm{e}^{-\mathrm{i}2\eta d} - \mathrm{i}\eta\mathscr{F}(d) - \mathscr{F}'(d)\right) & -\dfrac{\mathrm{i}k_{z,3}^3}{\rho_3\omega^2} \end{bmatrix}. \tag{62}$$